

# Effect of Cr and Fe Doping on the Structural and Optical Properties of ZnO Nanostructures

Prakash Chand, Anurag Gaur, Ashavani Kumar

**Abstract**—In the present study, we have synthesized Cr and Fe doped zinc oxide (ZnO) nanostructures ( $\text{Zn}_{1-\delta}\text{Cr}_\delta\text{Fe}_\text{b}\text{O}$ ; where  $\delta = a + b = 20\%$ ,  $a = 5, 6, 8 \text{ \& } 10\%$  and  $b = 15, 14, 12 \text{ \& } 10\%$ ) via sol-gel method at different doping concentrations. The synthesized samples were characterized for structural properties by X-ray diffractometer and field emission scanning electron microscope and the optical properties were carried out through photoluminescence and UV-visible spectroscopy. The particle size calculated through field emission scanning electron microscope varies from 41 to 96 nm for the samples synthesized at different doping concentrations. The optical band gaps calculated through UV-visible spectroscopy are found to be decreasing from 3.27 to 3.02 eV as the doping concentration of Cr increases and Fe decreases.

**Keywords**—Nanostructures, Optical Properties, Sol-gel method.

## I. INTRODUCTION

IN recent years, considerable interest has been focused on transition metal oxides as these are used in various applications because of their specific catalytic, optical, electrical and magnetic properties [1], [2]. The oxides of transition metals such as chromium, copper, zinc, iron, nickel and cobalt are an important class of semiconductors, which have applications in magnetic storage media, solar energy transformation, electronic, semiconductor, catalysis and electrical and optical switching devices [3], [4]. Among the oxides of transition metal, zinc oxide (ZnO) is considered to be one of the most important multifunctional semiconductor material for technological applications such as light emitting diodes, gas sensors, drug delivery, transparent field effect transistors, window layer for thin-film solar cells, transparent conducting electrodes, surface acoustic wave devices, piezoelectric devices, photodiodes and optoelectronic devices due to the wide band gap (3.37 eV), high transmission coefficient in the visible and near infrared spectral range and large excitation binding energy (60 meV) at room temperature [5], [6]. ZnO is also biodegradable, biocompatible and biosafe for medical and environmental applications. Moreover, ZnO has owned a giant potential commercially due to its low cost, non-toxic, abundant resources in the nature and environmental friendly. There are a wide variety of synthetic methods for the preparation of ultrafine oxide nanoparticles such as sol-gel, hydrothermal, microwave, solid state techniques and spray

pyrolysis methods etc [7]-[10]. Out of these methods, we prepared Cr and Fe doped zinc oxide (ZnO) nanostructures ( $\text{Zn}_{1-\delta}\text{Cr}_\delta\text{Fe}_\text{b}\text{O}$ ;  $\delta = a + b = 20\%$ , where  $a = 5, 6, 8 \text{ \& } 10\%$  and  $b = 15, 14, 12 \text{ \& } 10\%$ ) nanostructures by using sol-gel technique which is robust and reliable to control the shape and size of particles without requiring the expensive and complex equipments. Moreover, sol-gel process is a low temperature process. It means that less energy consumption and less pollution. Doping with selective elements offers an effective method to enhance and control the structural, electrical and optical properties of ZnO nanoparticles. Doping of various transition metals (e.g. Cr, Co, Ni, and Fe) in ZnO modify their structural and optical properties significantly. Among all TM dopant, chromium (Cr) and iron (Fe), due to its unique chemical stability, is recognized as one of the most efficient doping element to improve and tune the structural and optical properties of ZnO nanomaterials.

Therefore, in the present work, we report the effect of doping on the structural and optical properties of ZnO nanocrystals synthesized by sol-gel method at different doping concentrations of Cr and Fe ions. It is observed that the particle size of ZnO nanostructures increases while optical band gap decreases as we increase the doping concentrations of Cr and decrease the doping concentrations of Fe ions.

## II. EXPERIMENTAL

Cr and Fe doped zinc oxide (ZnO) nanoparticles ( $\text{Zn}_{1-\delta}\text{Cr}_\delta\text{Fe}_\text{b}\text{O}$ ; where  $\delta = a + b$ ;  $a = 5, 6, 8 \text{ \& } 10\%$  and  $b = 15, 14, 12 \text{ \& } 10\%$ ) has been synthesized by sol-gel method at different doping concentrations. A precursor solution for  $\text{Zn}_{0.80}\text{Cr}_{0.05}\text{Fe}_{0.15}\text{O}$  was prepared by dissolving high purity zinc nitrate ( $\text{Zn}(\text{NO}_3)_2 \cdot 6\text{H}_2\text{O}$ ), chromium nitrate ( $\text{Cr}(\text{NO}_3)_3 \cdot 9\text{H}_2\text{O}$ ) and Ferric nitrate ( $\text{Fe}(\text{NO}_3)_3 \cdot 9\text{H}_2\text{O}$ ) in de-ionized water under vigorous stirring and a 5M sodium hydroxide (NaOH) solution was then added drop wise with constant stirring to maintain the pH value at 12. The solution was magnetically stirred in electric oven for 5 hours. After that, the solution was allowed to cool down at room temperature. The solution was filtered and washed several times with de-ionized water and ethanol to remove the impurities ions and then centrifuged and dried at  $300^\circ\text{C}$  in furnace for 10 hrs. The same procedure was adopted to synthesize ZnO nanoparticles for remaining concentrations. The obtained ZnO powders were characterized by X-ray diffractometer (XRD; Rigaku Japan) with Cu-K $\alpha$  radiation source ( $\lambda = 1.54 \text{ \AA}$ ) for structural and phase purity analysis. XRD data were collected with a counting rate of  $2^\circ$  per minutes in the range of  $2\theta$  from  $20$  to  $80^\circ$ . The morphology and the structural characterization were conducted by Field

Prakash Chand is with the National Institute of technology, Kurukshetra, India-136119 (phone: +91-1744-233549; fax: +91-1744-238050; e-mail: KK\_PC2006@yahoo.com).

Anurag Gaur and Ashavani Kumar are with the National Institute of technology, Kurukshetra, India-136119 (e-mail: anuragdph@gmail.com, Ashavani@yahoo.com).

Emission scanning electron microscope (FESEM; FEG-Quanta-450, FEI). Photoluminescence (PL) and UV-visible spectra were measured at room temperature to study the optical properties of the synthesized ZnO nanostructures.

### III. RESULTS AND DISCUSSIONS

Fig. 1 shows the X-ray diffraction pattern (XRD) of Cr and Fe doped zinc oxide (ZnO) nanostructures synthesized at different doping concentrations. The corresponding X-ray diffraction peaks for (100), (002) and (101) planes confirm the formation of wurtzite structure of ZnO for all the samples. Although, we have observed impurity phases of ( $\text{ZnFe}_2\text{O}_4$ ,  $\text{Cr}_2\text{O}_3$ ,  $\text{Fe}_2\text{O}_3$ ,  $\text{FeO}$  and  $\text{CrO}_2$ ) in all the samples due to unreacted concentration of Cr/Fe and sintering effect. Furthermore, the line broadening of diffraction peaks (as observed from the Fig. 1) is an indication that the synthesized materials are in the nanometer range. The average crystallite size ( $D$ ) of ZnO nanostructures is calculated from the line broadening using Scherrer formula;  $D = K \lambda / \beta \cos \theta_B$ , where  $k = 0.89$  is the shape factor,  $\lambda$  is wavelength of  $\text{CuK}\alpha$  ( $1.54 \text{ \AA}$ ) radiation,  $\beta = B - b$ ,  $B$  is the full width at half maximum (FWHM),  $b$  represents the instrumental broadening and  $\theta_B$  is the angle of Bragg diffraction. The average crystallite size ( $D$ ) of ZnO nanostructures, calculated through Debye Scherrer formula, increases from 31 to 43 nm as the doping concentration of Cr increases and Fe decreases. In order to observe the structural morphology and size of the synthesized ZnO nanostructures, the samples were probed by high resolution field emission scanning electron microscope (FESEM).

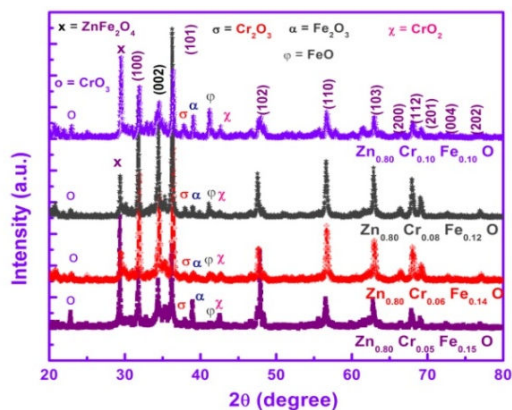


Fig. 1 XRD patterns of Cr and Fe doped ZnO nanostructures

Figs. 2 (a), (b) show the FESEM images of ZnO nanostructures synthesized at different doping concentrations of Cr and Fe ions. It is clear from FESEM images that the average particles size of ZnO nanostructures increases from 41 to 96 nm as the doping concentrations of Cr increases and Fe decreases. This also supports the XRD results that the particle size increases as the doping concentration of Cr increases and Fe decreases.

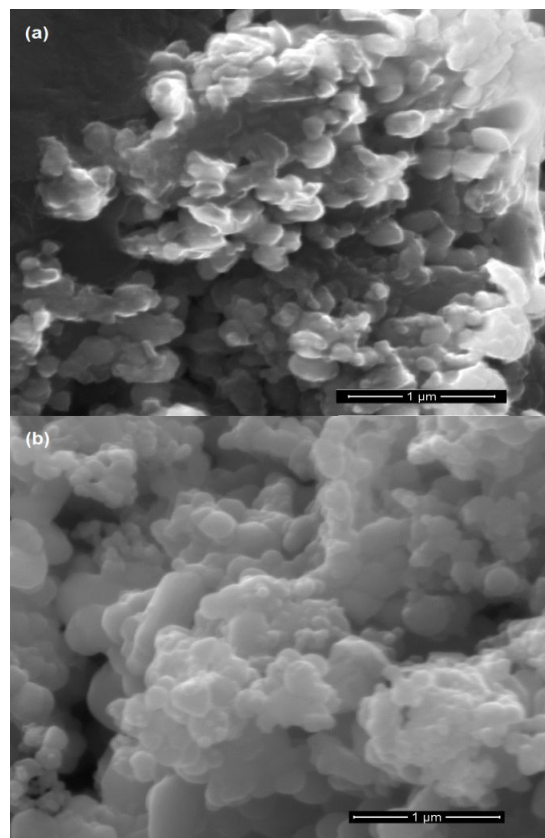


Fig. 2 FESEM images of ZnO nanostructures: (a)  $\text{Zn}_{0.80}\text{Cr}_{0.05}\text{Fe}_{0.15}\text{O}$  and (b)  $\text{Zn}_{0.80}\text{Cr}_{0.10}\text{Fe}_{0.10}\text{O}$

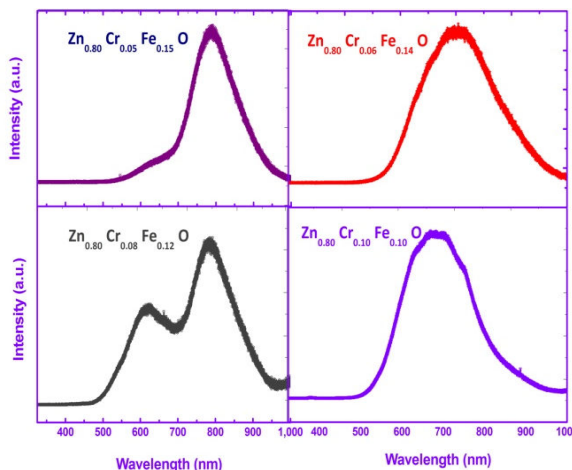


Fig. 3 Room temperature PL spectra of Cr and Fe doped ZnO nanostructures

Fig. 3 shows the room temperature PL spectra of Cr and Fe doped ZnO nanostructures. PL spectra were carried out using Xe light under the excitation of 325 nm for all the samples. The emission spectrums of the excitation at 325 nm give a broad visible emission. The broad visible emission from ZnO nanostructures may be due to the recombination of photogenerated holes with singly ionized charge states in

intrinsic defects such as oxygen vacancies, Zn interstitials, or impurities [11], [12].

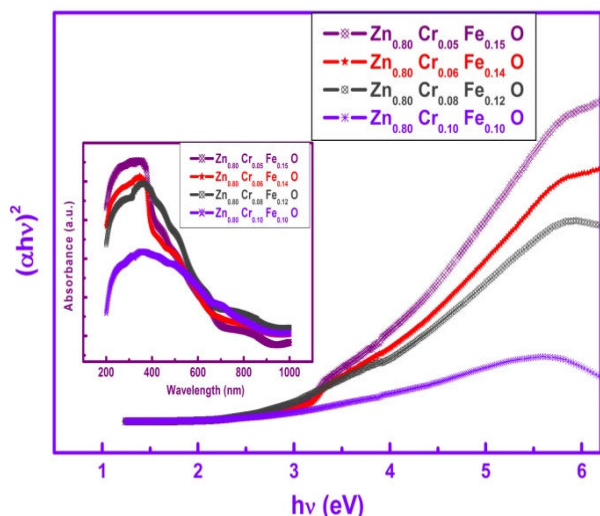


Fig. 4  $(\alpha hv)^2$  versus photon energy ( $h\nu$ ) plot of Cr and Fe doped ZnO nanostructures. The inset shows the absorbance versus wavelength plots

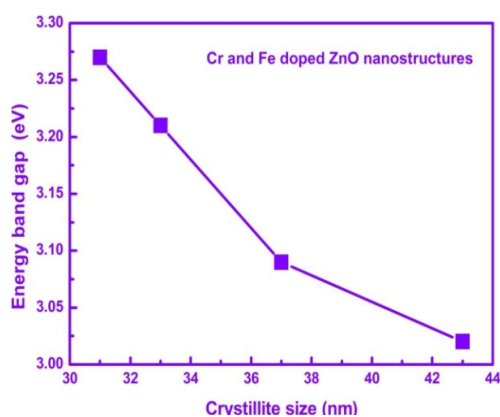


Fig. 5 Variation of crystallite size with energy band gap of Cr and Fe doped ZnO nanostructures

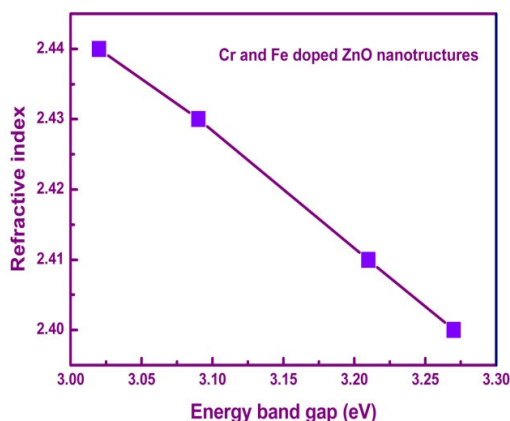


Fig. 6 Variation of energy band gap with refractive index of Cr and Fe doped ZnO nanostructures

The optical band gap energy of ZnO nanostructures for direct band gap is calculated by Tauc relation:  $(\alpha hv)^{1/n} = A(h\nu - E_g)$ , where  $E_g$  is the optical band gap,  $h\nu$  = photon energy,  $A$  is a constant,  $\alpha$  = absorption coefficient and  $n = 1/2$  for the allowed direct energy band and  $n = 3/2$  for a forbidden direct energy gap semiconductor [13], [14]. The absorption coefficient ( $\alpha$ ) can be calculated using the relation:  $\alpha = 4\pi k/\lambda$ ; where  $k$  is the absorption index or absorbance,  $\lambda$  is the wavelength in nm. The optical band gap energies ( $E_g$ ) is calculated by plotting Tauc's graphs between  $(\alpha hv)^2$  versus photon energy ( $h\nu$ ) and the intercept of this linear region on the energy axis at  $(\alpha hv)^2$  equal to zero gives the band gap. Fig. 4 shows the graph of  $(\alpha hv)^2$  versus photon energy ( $h\nu$ ) of Cr and Fe doped ZnO nanostructures. The inset of Fig. 4 shows the absorbance versus wavelength plots. The value of band gap of ZnO nanoparticles are 3.27, 3.21, 3.09, and 3.02 eV for the samples synthesized at different doping concentrations of Cr and Fe. The optical band gaps calculated through UV-visible spectroscopy are found to be decreasing from 3.27 to 3.02 eV as the doping concentration of Cr increases and Fe decreases. The decrease in optical energy band gap could be due to the increase of density of localized state in the conduction band. Fig. 5 shows the variation of crystallite size with energy band gap of Cr and Fe doped ZnO nanostructures. We have also calculated refractive index ( $n$ ) of Cr and Fe doped ZnO nanostructures using Moss relation [15]:  $n = \sqrt{\frac{k}{E_g}}$ ; where  $k$  is a constant with a value of 108 eV. For semiconducting materials refractive index play a significant role in determining the optical and electrical properties of the crystals and helps in the design of heterostructure laser, in optoelectronic devices as well as in solar cell applications [16]-[18]. Moreover, a correlation between refractive index ( $n$ ) and energy band gap ( $E_g$ ) has considerable bearing on the band structure of semiconductors and would be valuable in finding an adequate refractive index value of the unknown material from this relation. Fig. 6 shows the variation of energy band gap with refractive index of Cr and Fe doped ZnO nanostructures. It is observed from Fig. 6 that refractive index increases as the energy band decreases.

#### IV. CONCLUSIONS

We synthesized the Cr and Fe doped ZnO nanostructures via sol-gel method at different doping concentrations and studied their structural and optical properties. XRD shows the wurtzite phase formation in all samples with some impurities ( $ZnFe_2O_4$ ,  $Cr_2O_3$ ,  $Fe_2O_3$ ,  $FeO$  and  $CrO_2$ ) phases. FESEM analysis show that the average particle size of ZnO nanostructures increases from 41 to 96 nm as the doping concentration of Cr increases and Fe decreases. Photoluminescence spectra also confirm the phase formation of ZnO. It is observed that optical band gap decreased from 3.27 to 3.02 eV, and the refractive index ( $n$ ) increased from 2.40 to 2.44 as the doping concentration of Cr increases and Fe decreases.

## ACKNOWLEDGMENT

The authors would like thanks to Prof. Ravi Kumar and technical staff of Department of Material Science & Engineering, NIT Hamirpur for providing technical support during FESEM, PL and Raman measurements.

## REFERENCES

- [1] R. N. Nickolov, B. V. Donkova, K. I. Milenova, D.R. Mehandjiev, "Porous texture of CuO prepared from copper oxalate precursor," *Adsorpt. Sci. Technol.*, vol. 24, 2006, pp. 497-505.
- [2] P. K. Khanna, S. Gaikwad, P.V. Adhyapak, N. Singh, R. Marimuthu, "Synthesis and characterization of copper nanoparticles," *Mater. Lett.*, vol. 61, 2007, pp. 4711-4714.
- [3] J. Zhang, L. Zhang, X. Peng, X. Wang, "Fabrication of MgO nanobelts using a halide source and their structural characterization," *Appl. Phys. A*, vol. 73, 2001, pp. 773-775.
- [4] S. L. Pan, D. D. Zeng, H. L. Zhang, H. L. Li, "Preparation of ordered array of nanoscopic gold rods by template method and its optical properties," *Appl. Phys. A*, vol. 70, 2000, pp. 637-640.
- [5] L. Qian, Z. Liu, Y. Mo, H. Yuan, D. Xiao, "Large scale preparation of urchin like Li doped ZnO using simple radio frequency chemical vapor synthesis," *Mater. Lett.*, vol. 100, 2013, pp.124-126.
- [6] Z. L. Wang, "Splendid one-dimensional nanostructures of zinc oxide: A new nanomaterial family for nanotechnology," *ACS Nano*, vol. 2, 2008, pp.1987-92.
- [7] F. M. Judd, K. Iskandar, F. G. Okuyama, "Stable photoluminescence of zinc oxide quantum dots in silica nanoparticles matrix prepared by the combined sol-gel and spray drying method," *J. Appl. Phys.*, vol. 89, 2001, pp. 6431.
- [8] P. Chand, A. Gaur, A. Kumar, "Structural, optical and ferroelectric behavior of hydrothermally grown ZnO nanostructures," *Superlatt. Microstr.*, vol. 64, 2013, pp. 331-342.
- [9] S. Kamarnen, M. Bruno, E. Mariani, "Synthesis of ZnO with and without microwaves," *Mater. Res. Bull.*, vol. 35, 2000, pp. 1843-1847.
- [10] T. Tani, L. Madler, S. E. Pratsinis, "Homogeneous ZnO nanoparticles by flame spray pyrolysis," *J. Nanopart. Res.*, vol. 4, 2002, pp. 337-343.
- [11] Z.R. Khan, M.S. Khan, M. Zulfequar, M. Shahid Khan, "Optical and structural properties of ZnO thin films fabricated by sol-gel method," *Materials Sciences and Applications*, vol. 2, 2011, pp. 340-345.
- [12] Y.S. Kim, W.P. Tai, S.J. Shu, "Effect of Preheating Temperature on Structural and Optical Properties of ZnO thin films by sol-gel process," *Thin Solid Films*, vol. 491, No. 1-2, 2005, pp. 153-160.
- [13] N. Orhan, M. C. Baykul, "Characterization of size-controlled ZnO nanorods produced by electrochemical deposition technique," *Solid-State Electronics*, vol. 78, 2012, pp. 147-150.
- [14] P. Chand, A. Gaur, A. Kumar, "Structural and optical properties of ZnO nanoparticles synthesized at different pH values," *J. Alloys and Compounds*, vol. 539, 2012, pp. 174-178.
- [15] L. Hannachi, N. Bouarissa, "Band parameters for cadmium and zinc chalcogenide compounds," *Physica B*, vol.404, 2009, pp. 3650-3654.
- [16] Y. Akaltun, M.A. Yildirim, A. Ates, M. Yildirim, "The relationship between refractive index-energy gap and the film thickness effect on the characteristic parameters of CdSe thin films," *Optics Communications*, vol. 284, 2011, pp. 2307-2311.
- [17] N. Bouarissa, "Pseudopotential calculations of  $Cd_{1-x}Zn_xTe$ : Energy gaps and dielectric constants," *Physica B*, vol. 399, 2007, pp. 126-131.
- [18] F. Mezrag, W.K. Mohamed, N. Bouarissa, "The effect of zinc concentration upon optical and dielectric properties of  $Cd_{1-x}Zn_xSe$ ," *Physica B*, vol. 405, 2010, pp. 2272-2276.

Govt of India funded research project on Multiferroics. His other fields of working are Functional Nanostructured Oxides materials such as Double Perovskite based Magnetoresistive materials, Ferrites and Diluted Magnetic semiconductors. He has published more than thirty research papers in leading journals and reviewer of many International journals.

**Ashvani Kumar** is working as Professor and Head in the Department of Physics, National Institute of Technology, Kurukshetra. He did his Ph.D. in Physics from Aligarh Muslim University (AMU), Aligarh, India. He has completed D.S.T., Govt of India funded research project on high energy physics. He has published more than seventy research papers in international journals and reviewer of many International journals. His main research interests include radiation shielding and hadrontherapy using high Z particles as well as synthesis and characterization of nanomaterials for their applications in sensing devices like night vision cameras etc.

**Prakash Chand** is working as an Assistant Professor in Department of Physics, National Institute of Technology, Kurukshetra. His main researches interests include synthesis and characterization of transition metal oxides based nanostructures. He has published many research papers in leading journals and reviewer of International journals.

**Anurag Gaur** is working as an Assistant Professor in Department of Physics, National Institute of Technology, Kurukshetra. He did his Ph.D. degree from Indian Institute of Technology, Roorkee, India. He is also leading one D.S.T.,